

## FeCoSiN film with ordered FeCo nanoparticles embedded in a Si-rich matrix

Yan Liu,<sup>a)</sup> C. Y. Tan, Z. W. Liu, and C. K. Ong

Centre for Superconducting and Magnetic Materials, Department of Physics,  
National University of Singapore, 2 Science Drive 3, Singapore 117542, Singapore

(Received 3 October 2006; accepted 10 February 2007; published online 16 March 2007)

FeCoSiN film consisting of ordered arrays of FeCo nanoparticles embedded in a Si-rich matrix was fabricated on silicon substrate by reactive rf magnetron sputtering. These nanoparticles have a face-centered cubic structure and a mean diameter of  $\sim 7$  nm. The FeCoSiN film has a very high resistivity of up to  $1000 \mu\Omega$  cm due to the breakup of the metal continuum into isolated metal nanoparticles. The static and dynamic magnetic properties of the film were also investigated. A saturation magnetization of 1.0 T, coercivity of less than 5 Oe in both easy and hard axes, and anisotropy field of 27 Oe were obtained. The microwave permeability measurement showed a permeability of around 400 at low frequency and a ferromagnetic resonance frequency of about 1.1 GHz. © 2007 American Institute of Physics. [DOI: 10.1063/1.2714280]

Magnetic films are widely used in various fields of high-speed electronics. As data rates approach the gigahertz regime, a great deal of research effort<sup>1–13</sup> has been devoted to exploring films with high electrical resistivity in efforts to reduce eddy current loss. However, an increase in electrical resistivity will generally lead to a decrease in magnetization, which is undesirable. Among those researches, granular films consisting of magnetic metallic nanograins, typically Fe and Co, embedded in a nonmagnetic insulating matrix, have made important progress and a resistivity of  $500$ – $1000 \mu\Omega$  cm has been achieved.<sup>5</sup> Most of the granular films are deposited in an oxygen atmosphere, and further increase of resistivity requires higher oxygen concentration, which results in the oxidization of either Fe or Co, and therefore lower magnetization.<sup>5,11</sup> Furthermore, soft magnetic properties can only be obtained for the metal fractions within the metallic percolation, since otherwise the noninteracting assembly of particles may become superparamagnetic.<sup>7</sup> In this research, we added Si in FeCoN films and obtained a structure consisting of ordered arrays of FeCo nanoparticles embedded in a Si-rich matrix. This FeCoSiN film not only maintains the excellent soft magnetic properties of FeCoN film, such as high saturation magnetization, low coercivity, and high anisotropy,<sup>14</sup> but also has very high electrical resistivity of up to  $1000 \mu\Omega$  cm.

The FeCoSiN film was fabricated on a single-crystal silicon substrate with (100) surface orientation by reactive rf magnetron sputtering. A 2 in. Fe<sub>60</sub>Co<sub>40</sub> alloy disk with six pieces of Si chips ( $5 \times 10 \times 0.5$  mm<sup>3</sup>) was used as the sputtering target. A static magnetic field of about 120 Oe was applied parallel to the substrate surface during deposition to induce an in-plane magnetic anisotropy in the film. The sputtering chamber was evacuated to a base pressure of  $3 \times 10^{-7}$  Torr. An argon and nitrogen (3%) gas mixture was used as the ambient gas. During sputtering, the ambient gas pressure, the gas flow rate, and the rf power were maintained at 3.0 mTorr, 7 SCCM (SCCM denotes cubic centimeter per minute at STP), and 75 W, respectively. The thickness of the films was determined to be 100 nm from scanning electron

microscopy. The static magnetic property was measured using a *M-H* loop tracer. The resistivity at room temperature was obtained from standard four-point measurement. The microstructure was characterized by high-resolution transmission electron microscopy (HRTEM) using a JEOL JEM 3010 system, which is also equipped with an energy dispersive x-ray spectrometer. The permeability frequency spectrum up to 5 GHz was characterized by a shorted microstrip transmission-line perturbation method.<sup>15</sup>

The results from the transmission electron microscopy (TEM) characterization are shown in Fig. 1. The TEM image in Fig. 1(a) reveals that ordered arrays of nanoparticles are separated by an amorphous phase. The nanoparticles have a very small mean diameter of  $\sim 7$  nm and are separated by a distance of 1.5–7.5 nm from each other. This microstructure of FeCoSiN film is different from that of FeCoN film,<sup>14</sup> in which the nanoparticles appear to be interconnected with each other. The difference in the particle assembly between these two kinds of films is likely due to the presence of Si in FeCoSiN film. The selected area diffraction (SAD) pattern is shown in Fig. 1(c). Compared to the *d* spacing of FeCo face-centered cubic (fcc) lattice, a slightly larger *d*-spacing value is observed in our FeCoSiN film, indicating an expansion of the crystal lattice. Despite this expansion, the *d*-spacing values obtained from the SAD pattern of the FeCoSiN film can all be indexed to the FeCo fcc structure, indicating that the nanoparticles in the FeCoSiN film are fcc FeCo phase without Si impurity.

It is likely that Si preferentially combines with N, forming an amorphous SiN phase between the FeCo nanoparticles in the FeCoSiN film, since the binding enthalpy of Si with FeCo is about 290 kJ mol<sup>-1</sup> which is much less than that of Si with N, which is 470 kJ mol<sup>-1</sup> and the binding enthalpy of N with FeCo is below 50 kJ mol<sup>-1</sup> which is much less than that of Si with N.<sup>16</sup> From the HRTEM image in Fig. 1(b), *d* spacings of 2.10 and 1.82 Å corresponding to the (111) and (200) planes in FeCo fcc structure were identified. This fcc structure of the FeCoSiN film is different from that of the FeCoN film, in which the FeCo body-centered cubic (bcc) structure is dominant.<sup>14</sup> Therefore, based on the above finding from TEM images and in comparison with the FeCoN

<sup>a)</sup>Electronic mail: g0301187@nus.edu.sg

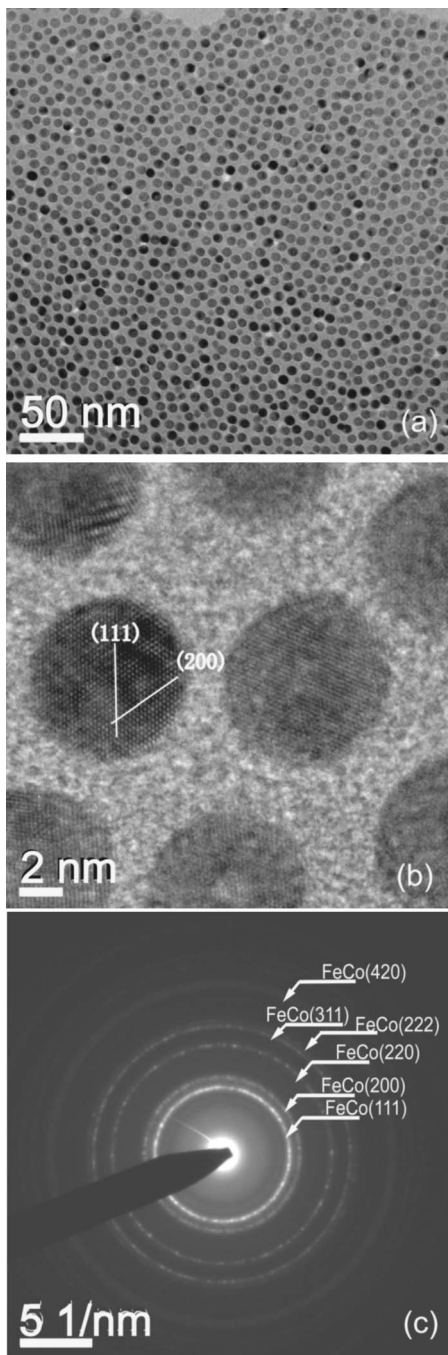


FIG. 1. (a) TEM image, (b) HRTEM image, and (c) SAD pattern of the FeCoSiN film.

film, we can deduce that the addition of Si caused the physical separation of the metal nanoparticles embedded in the Si-rich matrix and also modified the FeCo crystal structure from bcc to fcc structure.

The electric and magnetic properties of FeCoSiN film are summarized in Table I. For comparison, the properties for some other FeCo-based films are also presented. The resistivity ( $\rho$ ) of the FeCoSiN film is very high, up to  $1000 \mu\Omega \text{ cm}$ , whereas the resistivity of the  $\text{Fe}_{60}\text{Co}_{40}$  film is about  $100 \mu\Omega \text{ cm}$  and the addition of N into the film increases the resistivity of the  $\text{Fe}_{60}\text{Co}_{40}\text{N}$  film to about  $200 \mu\Omega \text{ cm}$ .<sup>14</sup> The extra addition of Si into the film greatly enhances the resistivity. In comparison, the addition of Al or Ta into the FeCo films only slightly increased the resistivity of the films.<sup>17,18</sup> Due to the addition of Si, the granular struc-

TABLE I. Magnetic and electric properties of some FeCo-based films.

Composition	$M_s$ (T)	$H_k$ (Oe)	$\rho$ ( $\mu\Omega \text{ cm}$ )	$\mu_{\text{in}}$	$f_r$ (GHz)
$\text{Fe}_{60}\text{Co}_{40}\text{N}^{\text{a}}$	1.8	40	200	560	2.4
FeCoSiN	1.0	27	1000	400	1.1
$\text{Fe}_{70}\text{Co}_{30}\text{N}^{\text{b}}$	2.17	...	160	...	...
$\text{Fe}_{49}\text{Co}_{34}\text{Ta}_{17}\text{N}^{\text{c}}$	1.12	46	189	240	2.04
$\text{Fe}_{46}\text{Co}_{34}\text{Al}_{20}\text{N}^{\text{c}}$	1.08	48	275	300	1.72

<sup>a</sup>Reference 14.

<sup>b</sup>Reference 17.

<sup>c</sup>Reference 18.

ture of FeCo nanoparticles embedded in a Si-rich matrix is formed. It is well known that in the metallic FeCo regime, the conductivity is determined by scattering of the electrons and the resistivity is low,<sup>19</sup> whereas in a (Si,N) rich dielectric regime, the conductivity is determined by the tunneling of electrons between isolated metal particles and the resistivity is high. Therefore, based on the microstructure of the FeCoSiN film, we can conclude that the breakup of the metal continuum into isolated metal nanoparticles plays an important role in the increase of the resistivity in the film. On the other hand, the Si concentration of our film is considered to be lower than that of common granular materials.<sup>6</sup> It is also very likely that some FeCo phases exist in the amorphous Si-rich matrix, as will be discussed later. Therefore, the electrical resistivity of the FeCoSiN thin film is still lower than that for the granular materials with giant magnetoresistance behavior.<sup>12</sup>

Figure 2 shows the hysteresis loop for the as-deposited FeCoSiN film. A very good combination of soft magnetic properties has been obtained with a saturation magnetization ( $M_s$ ) of 1.0 T, coercivity ( $H_c$ ) of less than 5 Oe in both easy and hard axes, and anisotropy field ( $H_k$ ) of 27 Oe. The observed room temperature ferromagnetism is believed to result from the exchange interaction between FeCo nanoparticles through the matrix with magnetic impurities. We had previously investigated the microstructure of FeCoN thin films without Si addition, sputtered at room temperature, and found that N occupies an interstitial site in the Fe or Co lattice to form different phases of FeCo and thus the amorphous phase existing in the FeCoN film is mostly FeCo due to deposition at the ambient temperature. This supports the presence of an FeCo amorphous magnetic phase in the Si-

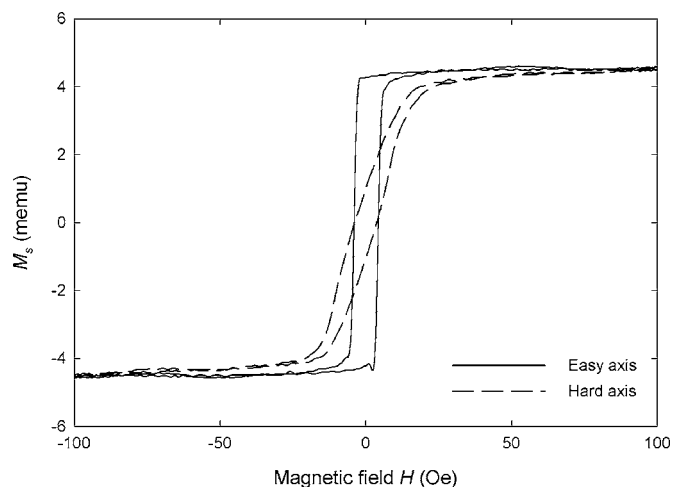


FIG. 2.  $M$ - $H$  loops of the FeCoSiN film.

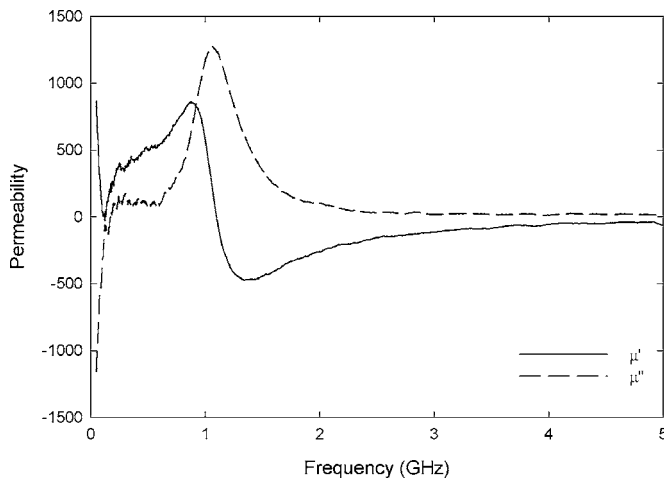


FIG. 3. Permeability spectrum of the FeCoSiN film.

rich matrix of our FeCoSiN film, which is also deposited at ambient temperature, although it is difficult to verify its content by conventional analysis methods. In addition, the exchange length<sup>20</sup>  $L_{\text{ex}} = \sqrt{A/K_1}$  (where  $A = 10^{-11} \text{ J m}^{-1}$  denotes the exchange stiffness and  $K_1 = 4 \times 10^3 \text{ J m}^{-3}$  the magneto crystalline anisotropy) is estimated to be  $\sim 50 \text{ nm}$  for Fe<sub>60</sub>Co<sub>40</sub> fcc structures, which is much larger than the FeCo nanoparticle size and the distance between the nanoparticles. Therefore, the nanoparticles can be exchange coupled with each other through the matrix with magnetic impurities. On the other hand, since the exchange interaction is weakened due to the separation of the nanoparticles in the FeCoSiN film, the anisotropy field decreased as well by taking the average of exchange interaction over several nanoparticles. Thus, the anisotropy field of the FeCoSiN film is smaller than that of the FeCoN film. The saturation magnetization also decreased due to Si addition because a nonmagnetic SiN phase forms between the nanoparticles. By assuming that the amorphous phase is totally nonmagnetic, the net magnetization of the metal particles is calculated to be 2.0 T if the volume of FeCo particles is considered to be 50% in our films. Provided that the lattice constant of fcc FeCo is 3.64 Å according to HRTEM results, each Fe or Co atom is calculated to contribute 2.0 bohr magnetons to the magnetization of the film. This is reasonably in accordance with the Slater-Pauling curve.<sup>21</sup> It is worth noting that a similar particle assembly was also found in CoPt nanoparticles with face-centered-tetragonal (fct) structure embedded in a Ag matrix,<sup>22</sup> which has a coercivity less than 100 Oe when as-deposited and is magnetically hard after annealing.

The high frequency properties were also investigated. Figure 3 shows the real and imaginary permeability spectra for the FeCoSiN film. The film has a ferromagnetic fre-

quency resonance of about 1.1 GHz, which is slightly less than the other FeCo-based films in Table I. The real permeability at low frequency is around 400, which is comparable to other soft magnetic films.

In summary, a structure consisting of ordered arrays of FeCo nanoparticles embedded in a Si-rich matrix has been obtained in the sputter-deposited FeCoSiN film. The addition of Si in the FeCoSiN film modified the crystal structure of FeCo nanoparticles from bcc to fcc structure and also led to a physical separation of the metal nanoparticles. The resistivity of the FeCoSiN film can be significantly enhanced to 1000  $\mu\Omega \text{ cm}$ , which is much higher compared to other FeCo-based films. FeCoSiN film established a way to not only fabricate high-resistivity FeCo-based films with tunable resistivity and magnetic properties by controlling the Si concentration but also to synthesize ordered arrays of ultrafine FeCo nanoparticles with potential for applications in nano self-assembly system.

- <sup>1</sup>M. Vroubel, Y. Zhuang, B. Rejaei, and J. Burghartz, *J. Magn. Magn. Mater.* **258**, 167 (2003).
- <sup>2</sup>S. X. Wang, N. X. Sun, M. Yamaguchi, and S. Yabukami, *Nature (London)* **407**, 150 (2000).
- <sup>3</sup>B. C. Webb, C. V. Jahnes, M. A. Russak, and M. E. Re, *J. Appl. Phys.* **69**, 5611 (1991).
- <sup>4</sup>Y. Shimada, M. Yamaguchi, S. Ohnuma, T. Itoh, W. D. Li, S. Ikeda, K. H. Kim, and H. Nagura, *IEEE Trans. Magn.* **39**, 3052 (2003).
- <sup>5</sup>S. Ohnuma and T. Masumoto, *Scr. Mater.* **44**, 1309 (2001).
- <sup>6</sup>S. Ohnuma, H. Fujimori, S. Mitani, and T. Masumoto, *J. Appl. Phys.* **79**, 5130 (1996).
- <sup>7</sup>G. S. D. Beach and A. E. Berkowitz, *IEEE Trans. Magn.* **41**, 2043 (2005).
- <sup>8</sup>S. S. Kim, S. T. Kim, J. M. Ahn, and K. H. Kim, *J. Magn. Magn. Mater.* **271**, 39 (2004).
- <sup>9</sup>K. Ikeda, K. Kobayashi, and M. Fujimoto, *J. Appl. Phys.* **92**, 5395 (2002).
- <sup>10</sup>C. A. Grimes, P. L. Trouilloud, J. K. Lumppp, and G. C. Bush, *J. Appl. Phys.* **81**, 4720 (1997).
- <sup>11</sup>S. Ohnuma, H. J. Lee, N. Kobayashi, H. Fujimori, and T. Masumoto, *IEEE Trans. Magn.* **37**, 2251 (2001).
- <sup>12</sup>M. Ohnuma, K. Hono, E. Abe, and H. Onodera, *J. Appl. Phys.* **82**, 5646 (1997).
- <sup>13</sup>H. Fujimori, S. Ohnuma, N. Kobayashi, and T. Masumoto, *J. Magn. Magn. Mater.* **304**, 32 (2006).
- <sup>14</sup>Y. Liu, Z. W. Liu, C. Y. Tan, and C. K. Ong, *J. Appl. Phys.* **100**, 093912 (2006).
- <sup>15</sup>Y. Liu, L. F. Chen, C. Y. Tan, H. J. Liu, and C. K. Ong, *Rev. Sci. Instrum.* **76**, 063911 (2005).
- <sup>16</sup>*CRC Handbook of Chemistry and Physics*, edited by D. R. Lide, 87th ed., Internet version (CRC, Boca Raton, FL, 1998), pp. 9–58.
- <sup>17</sup>H. Jiang, Y. J. Chen, and G. D. Lian, *IEEE Trans. Magn.* **39**, 3559 (2003).
- <sup>18</sup>V. Bekker, K. Seemann, and H. Leiste, *J. Magn. Magn. Mater.* **296**, 37 (2006).
- <sup>19</sup>H. L. Pinch, J. I. Gittleman, and B. Abeles, *Phys. Rev. Lett.* **35**, 247 (1975).
- <sup>20</sup>G. Herzer, *IEEE Trans. Magn.* **26**, 1397 (1990).
- <sup>21</sup>R. M. Bozorth, *Phys. Rev.* **79**, 887 (1950).
- <sup>22</sup>G. C. Hadjipanayis, *J. Magn. Magn. Mater.* **200**, 373 (1999).